Pulmonary Neovascularity: A Distinctive Radiographic Finding in Eisenmenger Syndrome

Ramon Sheehan, Joseph K. Perloff, Michael C. Fishbein, David Gjertson and Denise R. Aberle

Circulation 2005;112;2778-2785
DOI: 10.1161/CIRCULATIONAHA.104.509869
Circulation is published by the American Heart Association. 7272 Greenville Avenue, Dallas, TX 72514
 Print ISSN: 0009-7322. Online ISSN: 1524-4539

Pulmonary Neovascularity

A Distinctive Radiographic Finding in Eisenmenger Syndrome

Ramon Sheehan, MD; Joseph K. Perloff, MD; Michael C. Fishbein, MD; David Gjertson, PhD; Denise R. Aberle, MD

Background—We sought to characterize the distinctive pulmonary vascular abnormalities seen on chest radiographs and computed tomography (CT) scans in Eisenmenger syndrome.

Methods and Results—Thoracic CT scans, chest radiographs, and clinical data were reviewed for 24 Eisenmenger syndrome patients subdivided into those with interatrial (pretricuspid) versus interventricular or great arterial (posttricuspid) communications and in 14 acyanotic patients with pulmonary arterial hypertension (PAH) and no congenital heart disease. CT scans were scored blindly by 2 thoracic radiologists for the presence and severity of small, tortuous, intrapulmonary vessels, termed "neovascularity," lobular ground-glass opacification, and systemic perihilar and intercostal vessels. Histopathologic lung sections from 5 patients with Eisenmenger syndrome and from 3 patients with acyanotic PAH were reviewed. Associations between clinical and imaging features were tested by ANOVA and χ^2 tests. Kendall's rank-order coefficient and the Kruskal-Wallis test were used to test for significant differences in imaging features between Eisenmenger syndrome and acyanotic PAH. Neovascularity on chest radiographs was more common in Eisenmenger syndrome than acyanotic PAH, but differences were not significant. On CT, neovascularity, lobular ground-glass opacification, and hilar and intercostal systemic collaterals were more prevalent in Eisenmenger syndrome, with severity greater in posttricuspid communications. Three previously undescribed vascular lesions were identified histologically in Eisenmenger syndrome: malformed, dilated, muscular arteries within alveolar septa; congested capillaries within alveolar walls; and congested capillaries within the walls of medium-size, muscular pulmonary arteries. These lesions may correspond to the distinctive vascular abnormalities observed on chest radiographs and CT scans.

Conclusions—Distinctive vascular lesions on chest radiographs and CT scans in Eisenmenger syndrome appear to be correlated histologically with collateral vessels that develop more extensively with posttricuspid communications. **(*Circulation*. 2005;112:2778-2785.)**

Key Words: collateral circulation ■ heart defects, congenital ■ hypertension, pulmonary ■ lung ■ imaging

Heath and Edwards classified the histopathologic features of pulmonary hypertension in 1958.[1] Attention focused on 6 grades of structural abnormalities in muscular pulmonary arteries and arterioles. Plexogenic pulmonary arteriopathy, the most severe grade, was equally prevalent in Eisenmenger syndrome and primary pulmonary hypertension (PPH), 2 types of pulmonary vascular disease that could be distinguished by differences in elastic tissues of the pulmonary trunk and proximal pulmonary arteries.[2]

In Eisenmenger syndrome, we identified distinctive, micronodular, serpiginous opacities on chest radiographs and computed tomography (CT) scans and assigned the term "neovascularity" to these hitherto-undescribed lesions because they did not correspond to known patterns of pulmonary arterial, pulmonary venous, or collateral vascularity. The histopathology of these opacities and its relation to plexogenic pulmonary arteriopathy is unknown. Nor is it known why these distinctive vascular abnormalities occur in only some types of pulmonary hypertension.

We studied the distinctive vascular lesions on chest radiographs and chest CT scans in patients with Eisenmenger syndrome and in patients with acyanotic pulmonary artery hypertension (PAH) due to PPH or acquired forms of acyanotic PAH[2] and correlated our findings with clinical and histopathologic data. Different vascular patterns in pulmonary hypertension of different etiologies can be recognized on chest radiographs and CT scans. These patterns appear to be correlated with the histopathologic lesions that differ from Heath-Edwards plexogenic pulmonary arteriopathy.

Received November 24, 2004; revision received June 8, 2005; accepted July 29, 2005.

From the Division of Thoracic Imaging (R.S., D.R.A.), Department of Radiological Sciences; the Division of Cardiology (J.K.P.), Department of Medicine; and the Divisions of Surgical Pathology (M.C.F.) and Laboratory Medicine (D.G.), Department of Pathology and Laboratory Medicine, David Geffen School of Medicine at UCLA, Los Angeles, Calif.

Reprints requests to Denise R. Aberle, MD, Division of Thoracic Imaging, Department of Radiological Sciences, David Geffen School of Medicine at UCLA, 10833 Le Conte Ave, Los Angeles, CA 90095.1721. E-mail daberle@mednet.ucla.edu

Circulation **is available at http://www.circulationaha.org** **DOI: 10.1161/CIRCULATIONAHA.104.509869**

Methods

Patient Selection

Twenty-four consecutive adults, 10 men and 14 women aged 22 to 53 years (mean, 39±2), with unoperated cyanotic congenital heart disease were selected from the Ahmanson/UCLA Adult Congenital Heart Disease Center Registry after referral for CT pulmonary angiography performed between May 1994 and September 2000 in anticipation of lung transplantation. Six patients had >1 CT scan performed; in these cases, the analyzed scan was the 1 done closest to diagnostic echocardiography. Imaging data were also collected from 14 consecutive patients >18 years with acyanotic PAH, both primary and acquired forms, who had CT pulmonary angiography performed between April 1995 and September 1998 within 24 months of the diagnosis of PAH.

The congenital cardiac defects in Eisenmenger syndrome were established by transthoracic echocardiography with color flow imaging and Doppler interrogation performed on average within 6.0±7.1 months of the CT scans. Pulmonary hypertension in the patients with acyanotic PAH was established by transthoracic echocardiography and cardiac catheterization performed within 3.4±7.1 months of the CT scans.[3]

Age and sex data were secured from medical records. Systemic arterial oxygen saturation and hematocrit/hemoglobin values were recorded within 3 weeks of imaging studies. The UCLA institutional review board exempted this retrospective study from the approval process or patient informed consent.

Image Acquisition

Chest Radiographs

Upright posteroanterior and lateral chest radiographs were taken at a 72-inch source-to-image distance with high-kilovoltage techniques (110 to 140 kV) with various screen-film or computed radiography receptor systems of ≈200 speed.

CT Scans

CT pulmonary angiograms were obtained on either an Imatron Evolution electron beam CT (EBT) scanner (Imatron, Inc) or a GE HiSpeed CT/i scanner (General Electric Medical Systems). Scans were acquired at suspended maximal inspiration. Patients unable to breath-hold were preferentially studied at quiet respiration on the Imatron EBT scanner. Each study included an initial noncontrast sequence to exclude pulmonary vascular calcifications, followed by intravenous contrast-enhanced vascular sequences from 1 cm above the superior margin of the transverse aorta to 1 cm above the lower of the 2 hemidiaphragms.

Initial non–contrast-enhanced, continuous-volume datasets on the EBT scanner were acquired through the thorax according to a standardized protocol of 6-mm collimation, 6-mm table incrementation, and 300-ms exposure. Images were reconstructed with use of a high-spatial-frequency algorithm. Vascular sequences were performed in single-slice, continuous-volume mode with 3-mm collimation, 2-mm table incrementation, 100- to 200-ms exposure, and a standard reconstruction algorithm.

Studies acquired on the GE HiSpeed CT/i scanner consisted of an initial noncontrast sequence of 120 kV, 200 to 260 mA, 0.8- to 1.0-mm gantry rotation speed, 5-mm collimation, pitch of 1.5:1 to 2:1, 5-mm reconstruction interval, and a bone reconstruction algorithm. This was followed by a vascular sequence after administration of intravenous contrast of 3-mm collimation, pitch of 2:1, 2-mm reconstruction interval, and a standard reconstruction algorithm. Images were reviewed on softcopy with both mediastinal (width, 400 Hounsfield units [HU]; level, 40 HU) and lung (width, 1600 HU; level, −550 HU) window settings.

For all vascular sequences, a peripheral catheter was inserted into a large forearm or antecubital vein and avoiding introduction of air. Omnipaque 350 (Amersham Health) was administered by mechanical injection at standard flow rates of 3 to 4 mL/s, averaging 90 to 140 mL total. Vascular sequences were initiated 25 to 30 seconds after the start of the contrast bolus.

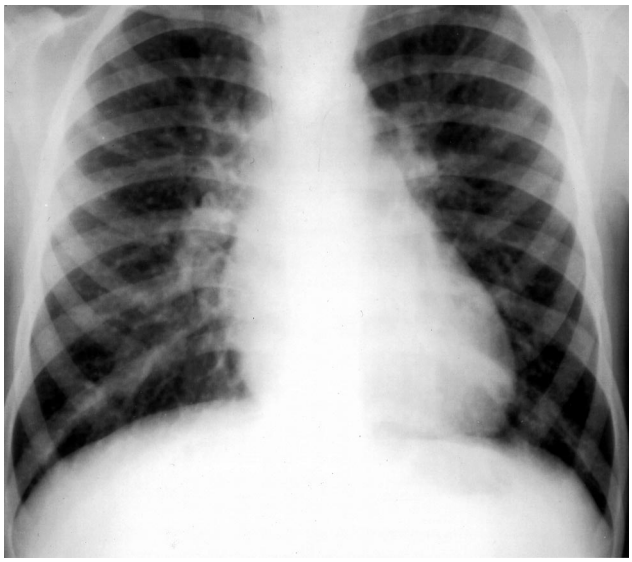

Figure 1. Chest radiograph of a 32-year-old man with a nonrestrictive VSD and Eisenmenger syndrome. Small, nodular opacities in the lungs correspond to pulmonary neovascularity grade 2. Enlarged central pulmonary arteries are indicative of PAH.

Image Interpretation

Two subspecialty-trained thoracic radiologists (R.S., D.R.A.) independently reviewed all chest radiographs and CT images. Both were aware that all patients were pulmonary hypertensive but were blinded to other clinical and histological data. Image analyses were standardized so that lung windows were reviewed first, enabling all relevant observations to be recorded before soft-tissue windows of the cardiac lesions were revealed. Chest radiographs and CT images were read in settings separated by at least 12 weeks to ensure that recall would not affect visual scoring. Scores were compared and inconsistencies reconciled by agreement after all images had been reviewed.

Chest radiographs and CT scans from 3 patients with cyanotic congenital heart disease outside the time period under consideration were used to establish visual standards for developing semiquantitative scoring systems for the presence and severity of specific imaging features by using principles developed for other visual scoring systems.[4] These visual standards contained features spanning the range of features being scored on the study images and were available for reference during image analysis. Chest radiographs were scored for the presence and severity of small, nodular opacities within the lungs on a 4-point, semiquantitative grading system: 0=no opacities, 1=opacities mildly pronounced, 2=opacities moderately pronounced, 3=opacities markedly pronounced (Figure 1). Similarly, CT scans were scored on a 4-point, semiquantitative grading system (0=absent, 1=mild, 2=moderate, 3=extensive) to determine the presence and severity of each of the following vascular patterns: (1) Neovascularity, defined as tiny, micronodular, serpiginous intrapulmonary vessels often in the subpleural lung or in proximity to centrilobular arterioles, coursing in directions inconsistent with known arteriolar anatomy (Figure 2A and 2B). (2) Lobular ground-glass, defined as hazy, increased lung attenuation at the center of secondary lobules fading to normal attenuation at the lobular margin (Figure 3). (3) Hilar collateral vessels, defined as small, serpiginous, vascular channels coursing in the carinal or bilateral hilar regions adjacent to mainstem, lobar, or interlobar arteries or bronchi (Figure 4). (4) Intercostal collaterals, defined as small, serpiginous, vascular channels coursing in chest wall soft tissues in proximity to pleural surfaces (Figure 5). These appeared as "beading" along the visceral pleural margin and occasionally entered the lung to join intrapulmonary vessels, forming serpiginous neovascularity in the lung periphery (Figure 6A and 6B). Intercostal vessels had to be increased in number to be judged abnormal.

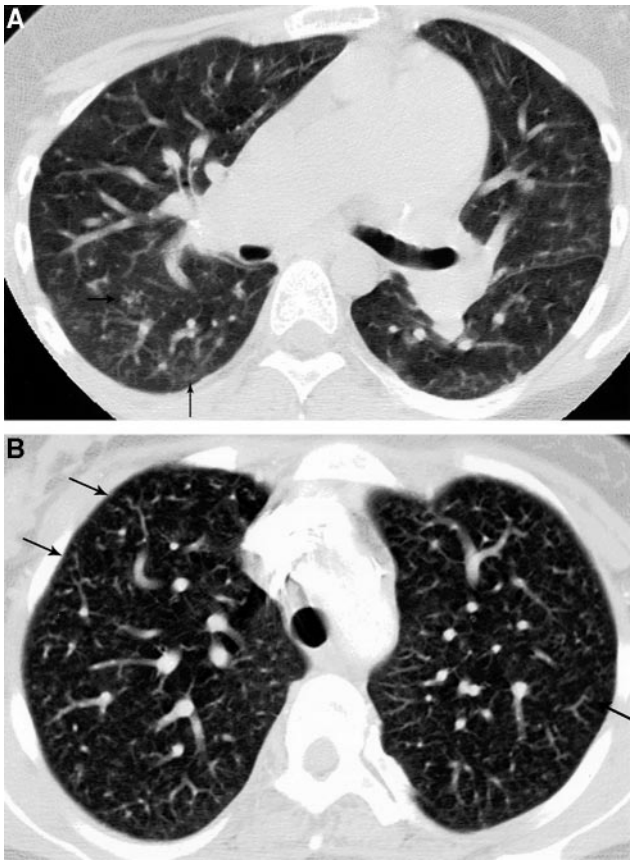

Figure 2. A, Axial CT scan with lung windows in a 26-year-old woman with Eisenmenger syndrome and double-outlet right ventricle. Numerous micronodules are in continuity with peripheral pulmonary arteries (arrows) and correspond to grade 3 neovascularity. B, Axial CT scan with lung windows in a 35-year-old woman with Eisenmenger syndrome, complete transposition of the great arteries, and a nonrestrictive VSD. Numerous small, serpiginous neovessels appear within the lungs (arrows) as grade 3 neovascularity.

Neovascularity and lobular ground-glass were scored on lung windows, whereas collateral vessels were scored on soft-tissue windows. Pulmonary artery thrombus, recanalized thrombus, pulmonary artery mural calcifications, and incidental cardiopulmonary findings were recorded as present or absent.

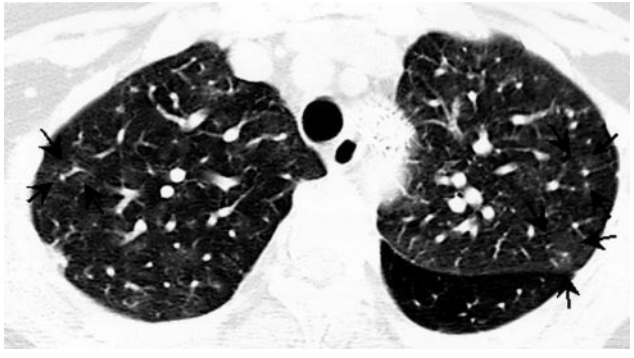

Figure 3. Axial CT scan with lung windows in a 42-year-old man with Eisenmenger syndrome and a nonrestrictive VSD. A distinctive, hazy, lobular, ground-glass pattern with increased attenuation appears at the center of secondary lobules (arrows), fading at the margins.

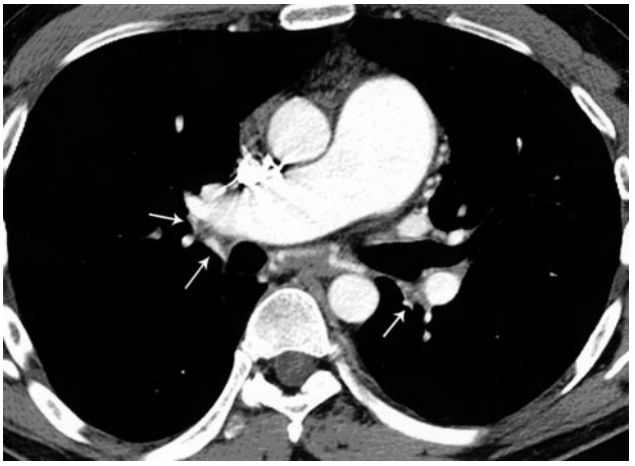

Figure 4. Soft-tissue windows of a CT scan in a 28-year-old woman with Eisenmenger syndrome and a nonrestrictive VSD. Multiple small, hilar vessels course in the subcarinal and bilateral hilar regions (arrows) adjacent to bronchovascular bundles.

Histopathology

Histological material was studied from 5 patients with Eisenmenger syndrome, 1 with an ostium secundum atrial septal defect (ASD) and 4 with posttricuspid lesions, and in 3 patients with acyanotic PPH. The lung specimens from patients with PPH were obtained during surgery for lung transplantation, whereas Eisenmenger syndrome specimens were obtained at necropsy.

Lung specimens were fixed in formalin and embedded in paraffin. Sections of 5-μm thickness were stained with hematoxylin-eosin for light microscopy. All sections were analyzed for the following vascular lesions: (1) medial hypertrophy, (2) intimal proliferation, (3) plexiform lesions, and (4) vascular dilatation lesions. Vascular lesions not corresponding to these patterns were specifically recorded. All specimens were reviewed by the same cardiopulmonary pathologist (M.C.F.). The number of vascular lesions was scored on individual histological sections according to the same 4-point, semiquantitative grading system used to grade vascular lesions on CT. Systematic sampling or scoring throughout the lungs was not possible, nor was it possible to correlate lung specimens directly with in vivo CT image data.

Figure 5. Soft-tissue windows of a contrast-enhanced CT scan in a 50-year-old man with Eisenmenger syndrome and a nonrestrictive VSD. Multiple bilateral, intercostal, collateral vessels appear along the posterior and right lateral chest walls (arrows).

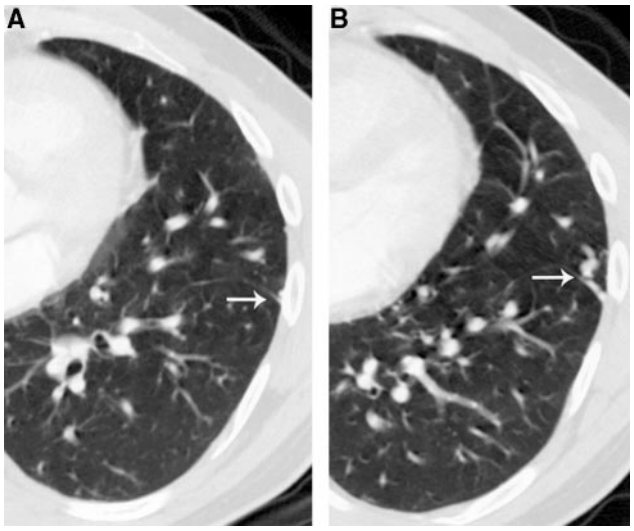

Figure 6. A and B, Lung windows of a CT scan in a 36-year-old man with Eisenmenger syndrome and a nonrestrictive VSD. Small extrapulmonary, left chest wall vessels are in continuity with peripheral pulmonary vessels. A, The left chest wall vessels appear as "beading" along the lateral pleural surface (arrows) and B, penetrate the lung to connect with small serpiginous, intrapulmonary neovessels.

Statistical Methods

Associations between individual chest radiographic or CT findings and age, sex, systemic arterial oxygen saturation, hematocrit, and hemodynamic data were tested by ANOVA and a χ^2 test for continuous and categorical variables, respectively. To assess for significant differences in chest radiographic and CT findings between patients with Eisenmenger syndrome versus acyanotic PAH, Kendall's rank-order correlation coefficient (τ_b) was computed, and the Kruskal-Wallis test was applied to the ordinal data. To highlight differences, semiquantitative scores for chest radiographic and CT features for each group were also dichotomized in 2 ways: (1) negative (grade 0) versus positive (grades 1 to 3) and (2) mild (grade 1) versus extensive (grades 2 and 3). All probability values were 2 sided; after allowing for multiple comparison via Bonferroni adjustment, statistical significance was set at $P<0.004$.

To analyze differences in CT features in Eisenmenger syndrome, these patients were further subdivided into those with pretricuspid lesions[5,6] versus those with posttricuspid lesions (ventricular septal defects [VSDs] and/or great arterial communications). Because of the small numbers of patients, results were expressed as percentages along with exact (binomial) 95% confidence intervals (CIs); tests of significance for proportions among comparative grades were not done. Because correlations between histological data and the CT image data were not possible, no attempt was made to analyze the histological data for statistical significance.

Results

Clinical Features

Among 24 patients with Eisenmenger syndrome, echocardiography disclosed a pretricuspid lesion (ostium secundum ASD) in 7 patients and posttricuspid lesions in 17, including VSD in 9, truncus arteriosus in 2, and 1 each with patent ductus arteriosus (PDA), PDA with ASD, VSD with PDA, double-outlet right ventricle with VSD, complete transposition of the great arteries with VSD/ASD/PDA, and endocardial cushion defect with nonrestrictive VSD. The 7 patients with pretricuspid lesions were believed to represent the coincidence of PPH and ASD or stretched patent foramen ovale.[5,6]

Transcutaneous systemic arterial oxygen saturations in Eisenmenger syndrome ranged from 68% to 87% (mean, 78±6%), and iron-replete hematocrit levels (Beckman Coulter Inc) ranged from 58 to 71 gm/dL (mean, 64±4). Right ventricular systolic pressures by echocardiography were at systemic level in Eisenmenger syndrome patients with posttricuspid lesions; right ventricular/pulmonary artery systolic pressures ranged from 102 to 138 mm Hg in those with pretricuspid lesions.

The 14 patients with acyanotic PAH included 2 men and 12 women aged 20 to 76 years (mean, 44±4). Eight of 14 met the clinical and echocardiographic criteria for PPH.[5] The remaining 6 patients had acquired pulmonary hypertension caused by systemic or parenchymal disease, including 2 with chronic obstructive pulmonary disease, 2 with systemic lupus erythematosus, 1 with chronic thromboembolic disease, and 1 with portal hypertension. Transcutaneous systemic arterial oxygen saturation in the 14 patients with acyanotic PAH was ≥96%, hematocrits ranged from 33 to 44 mg/dL (mean, 37±2), and echocardiographic right ventricular systolic pressures ranged from 42 to 118 mm Hg (mean, 83±9).

There were no significant associations between chest radiographic or CT features and age, sex, systemic arterial oxygen saturation, hematocrit, or right ventricular systolic pressure in the 2 major groups (Eisenmenger syndrome and acyanotic PAH).

Chest Radiographic Findings

Chest radiographs were available for review in 26 patients. Small, nodular, vascular opacities were visible on chest radiographs of 12 of 17 (71%) with Eisenmenger syndrome and 3 of 9 (33%) with acyanotic PAH, but the difference was not significant (Table 1).

TABLE 1. Frequency and Extent of Nodular Opacities on Chest Radiographs (N=26*)

	Radiographic Grading					Patients Graded as Positive	Patients Graded as Severe
Patient Category	0	1	2	3	Correlation†	(Grades 1–3)	(Grades 2 and 3)
Acyanotic PAH	6	3	0	0	0.43±0.13 (P=0.02)	3/9 (33%)	0/9 (0%)
Eisenmenger syndrome	5	4	5	3		12/17 (71%)	8/17 (47%)

Numbers in parentheses represent percentages of total positive.

*Chest radiographs were available for 26 of the 38 patients.

†Kendall's τ_b along with its asymptotic SE. The P value from the Kruskal-Wallis test of equal proportions of grading ranks is presented parenthetically. Statistical significance was $P<0.004$.

TABLE 2. Frequency and Extent of CT Abnormalities Among Patients (N=38)

CT Observation	CT Score of Extent 0	1	2	3	Correlation*	Patients Graded as Positive (Grades 1–3)	Patients Graded as Severe (Grades 2 and 3)
Nodular, serpiginous pulmonary vessels							
Acyanotic PAH	11	2	1	0	0.68±0.08 ($P<0.001$)	3/14 (21%)	1/14 (7%)
Eisenmenger syndrome	1	7	4	12		23/24 (96%)	16/24 (67%)
Pretricuspid (ASD)	1	5	0	1		6/7 (86%)	1/7 (14%)
Posttricuspid	0	2	4	11		17/17 (100%)	15/17 (88%)
Lobular ground-glass							
Acyanotic PAH	13	0	1	0	0.48±0.11 ($P=0.002$)	1/14 (7%)	1/14 (7%)
Eisenmenger syndrome	9	9	1	5		15/24 (62%)	6/24 (25%)
Pretricuspid (ASD)	3	4	0	0		4/7 (57%)	0/7 (0%)
Posttricuspid	6	5	1	5		11/17 (65%)	6/17 (35%)
Hilar and intercostal collaterals							
Acyanotic PAH	6	5	2	1	0.65±0.09 ($P<0.001$)	8/14 (57%)	3/14 (21%)
Eisenmenger syndrome	0	4	3	17		24/24 (100%)	20/24 (83%)
Pretricuspid (ASD)	0	2	0	5		7/7 (100%)	5/7 (71%)
Posttricuspid	0	2	3	12		17/17 (100%)	15/17 (88%)

Numbers in parentheses represent percentages of total positive.

*Kendall's τ_b along with its asymptotic SE. The P value from the Kruskal-Wallis test of equal proportions of grading ranks is presented parenthetically. Statistical significance was $P<0.004$.

CT Findings

Overall, the CT features of neovascularity, lobular ground-glass, and hilar/intercostal collaterals differed significantly between patients with Eisenmenger syndrome and those with acyanotic PAH, being present more commonly and with greater severity in Eisenmenger syndrome (correlations equaled 0.68, 0.48, and 0.65, respectively' Table 2).

Neovascularity was present on CT scans in 23 of 24 (96%) of Eisenmenger patients and in 3 of 14 (21%) of acyanotic PAH patients (Table 2). Moreover, among Eisenmenger patients, neovascularity was more severe (grade 2 or 3) in posttricuspid lesions (15/17, or 88%; 95% CI, 64% to 89%) than in pretricuspid lesions (1/7, or 14%; 95% CI, 0% to 58%).

Lobular ground-glass was a CT feature in 15 of 24 patients (62%) with Eisenmenger syndrome versus only 1 of 14 patients (7%) with acyanotic PAH (Table 2). When Eisenmenger syndrome patients were subdivided, the magnitude of this difference was unchanged: lobular ground-glass of any severity (grades 1 to 3) was seen in 11 of 17 patients (65%; 95% CI, 38% to 86%) with posttricuspid lesions and in 4 of 7 patients (57%; 95% CI, 18% to 90%) with pretricuspid lesions. Severe grades of lobular ground-glass were found in 0 of 7 (0%; 95% CI, 0% to 41%) and 6 of 17 (35%; 95% CI, 14% to 62%) Eisenmenger syndrome patients with pretricuspid and posttricuspid lesions, respectively.

There were significantly increased numbers of small perihilar and intercostal collaterals in all Eisenmenger syndrome patients and in 8 of 14 (57%) patients with acyanotic PAH (Table 2). Again, the more severe grades of collaterals (grades 2 and 3) were more common among Eisenmenger syndrome patients with posttricuspid lesions (15/17, or 88%; 95% CI, 64% to 98%) than in those with pretricuspid lesions (5/7, or 71%; 95% CI, 29% to 96%). There was no significant relation between the presence and severity of hilar or intercostal collaterals and the presence and severity of neovascularity or lobular ground-glass (data not shown).

Histological Observations

Three patients with acyanotic PPH from whom histological material was available had medial hypertrophy and intimal proliferation but no plexiform lesions. There was a large, recanalized thrombus within the proximal pulmonary arteries in 1 patient.

Medial hypertrophy and intimal proliferation were present in 3 of 5 Eisenmenger syndrome patients. Classic plexiform lesions corresponding to Heath-Edwards grade 4 were identified in specimens from 3 patients (Figure 7), and vascular dilatation and advanced lesions of plexiform pulmonary arteriopathy were present in all 5 Eisenmenger syndrome patients.

In Eisenmenger syndrome, 3 previously undescribed vascular lesions were identified by light microscopy. Two of the lesions involved abnormal capillaries. The first consisted of numerous dilated, congested capillaries within adventitial tissue surrounding medium-size, muscular, pulmonary arteries (Figure 7A). The second consisted of markedly dilated, congested capillaries within alveolar tissues (Figure 7B). The third lesion, which consisted of clusters of abnormally dilated, tortuous, muscular arteries within alveolar septa (Figure 7C), was visible on slide preparations without magnification and appeared to represent the small, tortuous, neovascularity vessels observed on CT. Figure 7D shows a plexiform lesion of hypertensive pulmonary arteriopathy.

Discussion

The histological types of pulmonary vascular disease described by Heath and Edwards are equally prevalent in

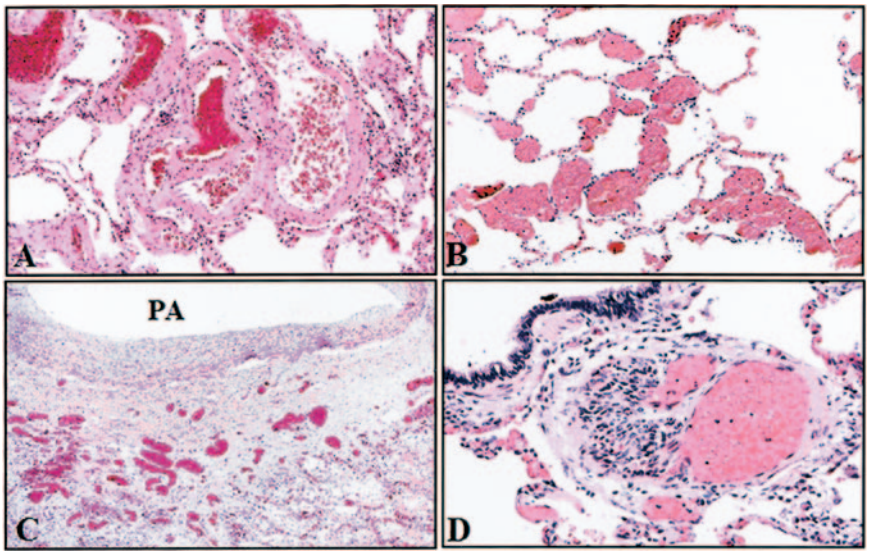

Figure 7. Microscopic sections from a man with Eisenmenger syndrome and a nonrestrictive VSD. A, Clusters of dilated, tortuous, muscular arteries within alveolar septa, the latter of which were visible without magnification and resembled the neovessels observed on CT. B, Markedly dilated, congested capillaries within the alveolar tissues. C, A markedly dilated, vascular lesion consisting of congested capillaries within the adventitial tissue surrounding a medium-size, muscular, pulmonary artery (PA). These lesions differed distinctly from plexiform lesions of hypertensive pulmonary arteriopathy (D), with dilated channels and foci of prominent endothelial proliferation (all H&E stain, original magnifications: A=×100, B=×200, C=×40, D=×400.

Eisenmenger syndrome and acyanotic PAH.[1,7–13] The distinctive radiographic neovascularity lesions described herein are significantly more frequent in Eisenmenger syndrome and are most severe in Eisenmenger syndrome with posttricuspid right-to-left shunts at the ventricular or great arterial level. Chest radiographs disclosed distinctive nodular opacities within the lungs. On CT, neovascularity appeared as small, nodular, and serpiginous vessels in the lung periphery, occurring in conjunction with lobular ground-glass opacification. In Eisenmenger syndrome, increased systemic arterial collateral vessels were seen in the hilar and intercostal regions; the intercostal vessels sometimes penetrated the lung and contributed to neovascularity.

In Eisenmenger syndrome, we report previously undescribed histological vascular lesions characterized by marked capillary dilatation and congestion in alveolar spaces and in the adventitial tissue surrounding small, muscular arteries. Abnormal clusters of small, muscular arteries were visible within the alveolar walls without magnification and had the distinctive serpiginous morphology of neovascularity seen on CT. Although direct radiological/histopathologic confirmation was not possible, the distinctive neovascularity lesions suggest collateralization around tiny resistance vessels rather than Heath-Edwards lesions of plexogenic pulmonary arteriopathy. Lobular ground-glass may be an indirect reflection of collateral flow below the limits of macroscopic resolution, correlating with dilated capillary networks in alveolar spaces.

Systemic-to-pulmonary vascular collaterals have long been known[14–18] and primarily involve bronchial arteries that nourish the airways and serve as vasa vasorum for pulmonary arteries. More controversial has been the role of the systemic circulation in providing precapillary and capillary bronchopulmonary anastomoses, although necropsy studies with current 3-dimensional, computer-aided techniques have disclosed different types of collaterals in the lungs of patients with cyanotic congenital heart disease.[18] Systemic collateral channels develop at various levels in the pulmonary circulation, depending on hemodynamic circumstances, and may serve as tiny compensatory pathways downstream from obstructive pulmonary vascular disease or as bypass channels that divert flow from proximal prestenotic lesions to distal dilation lesions and alveolar capillaries.[18]

The development of systemic-to-pulmonary collaterals may vary according to the timing and severity of pulmonary vascular disease. Pretricuspid and posttricuspid communications in Eisenmenger syndrome have different pathophysiological and hemodynamic consequences[19–21] that may account for the significant differences in the degrees of neovascularity and lobular ground-glass appearance. In normal fetuses, a nonrestrictive ductus arteriosus equalizes pulmonary arterial, systemic arterial, and right and left ventricular systolic pressures. This equalization of pressures persists in infants with nonrestrictive posttricuspid defects, so the direction of shunt flow depends on the relative resistances in the pulmonary and systemic vascular beds. At birth, pulmonary vascular resistance falls precipitously to systemic levels and then continues to fall during the next few months. As resistance falls, the magnitude of a left-to-right shunt increases. Survival then depends chiefly on curtailment of excessive pulmonary flow by the development of pulmonary vascular disease. Adults with nonrestrictive posttricuspid lesions have, by definition, pulmonary hypertension at systemic levels, but it is suprasystemic pulmonary vascular resistance that reverses the shunt, diminishes pulmonary arterial blood flow, and stimulates formation of systemic collateral circulation to the lung parenchyma. Conversely, nonrestrictive pretricuspid defects are not accompanied by pulmonary vascular disease, reversed shunt, and diminished pulmonary blood flow and do not stimulate formation of systemic collaterals to the lung parenchyma. The magnitude and direction of shunts do not depend on systemic and pulmonary vascular resistances but on the relative compliances of the right and left ventricles, which are similar in utero and at birth but then diverge as left ventricular mass exceeds right ventricular mass during the process of normal extrauterine growth. Left-to-right shunt flow awaits this regression of right ventricular mass and increase in compliance, a time course that permits the pulmonary bed to evolve

into a low-pressure, low-resistance circulation. When a left-to-right shunt is then established, pulmonary arterial pressure remains normal within a low-resistance compliant vascular bed. Eisenmenger syndrome is uncommon in patients with a nonrestrictive ASD because pulmonary vascular disease is an unlikely sequel of increased flow into a low-pressure, low-resistance pulmonary circulation. Accordingly, it has been proposed that Eisenmenger syndrome in adults with an ASD represents the coincidence of the interatrial communication and PPH.[6]

Neovascularity and lobular ground-glass were significantly more common in Eisenmenger syndrome than in acyanotic PAH and were more common with posttricuspid defects in which pulmonary vascular disease developed early in life. Because our patients were adults, we do not know at what age neovascularity first becomes manifest.

Certain alternative explanations for the increased lung attenuation in Eisenmenger syndrome can be discounted. Pulmonary venous hypertension and pulmonary edema result in vascular redistribution (arterial and venous), together with interstitial edema, peribronchial cuffing, indistinct perihilar vessels, septal lines, thickening of fissures, and pleural effusions. Pulmonary edema may appear as increased lung attenuation on CT but is usually in a bronchovascular or gravity-dependent distribution and does not exhibit the distinctive central pattern within individual lobules that we observed.

Intrapulmonary hemorrhage, also relatively common in Eisenmenger syndrome, appears on chest radiographs and CT scans as transitory single or multiple confluent, segmental areas of ground-glass attenuation or consolidation.[22–24] Conversely, neovascularity and lobular ground-glass attenuation were permanent features in those patients in whom serial scans were available for review.

Lobular ground-glass can be mistaken for mosaic attenuation, which is common with chronic thromboembolism and other noncardiac causes of pulmonary hypertension.[25] However, the lobular ground-glass that we observed had characteristic high attenuation at the center of the pulmonary lobule and normal attenuation at the lobular margin contiguous with the interlobular septum, and the distribution of lobular ground-glass was relatively diffuse. In contrast, mosaic perfusion appears as geographic regions, or clusters, of lobules of uniform increased attenuation alternating with lobules of decreased attenuation. In an individual lobule, attenuation is homogeneous and does not taper peripherally at the septal margin. Increased attenuation in mosaic perfusion reflects regions of normal or hyperperfused lung supplied by the remaining pulmonary circulation. We postulate that the lobular ground-glass in Eisenmenger syndrome represents centrilobular perfusion by small, systemic-to-pulmonary collaterals at or below the arteriolar level.

Increased numbers of systemic arterial collaterals in the carinal, hilar, and intercostal regions on CT were universal in Eisenmenger syndrome but were significantly less frequent in acyanotic PAH. Intercostal vessels entered the lung directly across the costal pleura in Eisenmenger syndrome. There was no significant correlation between CT observations of systemic collaterals and either lobular ground-glass or neovascularity.

The retrospective design of our study created some limitations. Selection was based on referral for cross-sectional imaging, usually in anticipation of lung transplantation or for evaluation of chronic pulmonary thromboembolism. Because the study groups were not matched for demographic variables, unintentional selection bias might have been introduced. The retrospective design precluded direct correlation between CT and histological data. Neovascularity on CT strikingly resembled the histology of dilated, tortuous, muscular arteries clustered within alveolar tissues, but direct correlation would have been required to be certain that these CT and histological findings represented the same lesion. Finally, our analysis involved relatively few patients, which limits our ability to confirm the significance of differences between Eisenmenger patients with pretricuspid and posttricuspid lesions.

In conclusion, we report distinctive features on chest radiographs and CT scans that were significantly more common in Eisenmenger syndrome than in acyanotic PAH patients. On CT, neovascularity, lobular ground-glass, and increased systemic collaterals were identified regardless of the etiology of PAH, although they were significantly more common in Eisenmenger syndrome. Neovascularity and ground-glass opacification were more prevalent and more severe in posttricuspid defects in which pulmonary hypertension was present early in life, suggesting that the lesions were influenced by time of onset and duration of pulmonary vascular disease.

Histological material from patients with Eisenmenger syndrome revealed typical plexiform lesions as well as previously undescribed vascular abnormalities: Malformed, tortuous vessels, and dilated, congested capillaries within alveolar septae and the pulmonary arterial adventitia. We postulate that these lesions can be correlated with the CT findings of neovascularity and lobular ground-glass, respectively, and that they are manifestations of tiny collaterals that develop primarily in the lungs of patients with Eisenmenger syndrome.

Acknowledgments

The authors thank Eric M. Hart, MD, and Melanie Greaves, MD, for supervising and interpreting many of the original CT scans as well as John S. Child, MD, who performed all echocardiographic examinations in these patients.

References

1. Heath D, Edwards JE. The pathology of hypertensive pulmonary vascular disease: a description of six grades of structural changes in the pulmonary arteries, with special reference to congenital cardiac septal defects. *Circulation*. 1958;18:533–547.
2. Wagenvoort CA, Wagenvoort N. Pathology of the Eisenmenger syndrome and primary pulmonary hypertension. *Adv Cardiol*. 1974;11:123–130.
3. Child JS. Transthoracic and transesophageal echocardiographic imaging: anatomic and hemodynamic assessment. In: Perloff JK, Child JS. *Congenital Heart Disease in Adults.* 2nd ed. Philadelphia: WB Saunders Co; 1998:91–128.
4. International Labour Office (ILO). *Guidelines for the Use of the ILO International Classification of Radiographs of Pneumoconioses, Revised Edition 2000 (Occupational Safety and Health Series, No. 22).* Geneva: International Labour Office; 2002.

5. Archer S, Rich S. Primary pulmonary hypertension. *Circulation*. 2000; 102:2781–2791.
6. Perloff JK. Atrial septal defect: simple and complex. In: Perloff JK. *Clinical Recognition of Congenital Heart Disease*, 5th ed. Philadelphia: WB Saunders Co; 2003:233–299.
7. Edwards JE. Functional pathology of the pulmonary vascular tree in congenital heart disease. *Circulation*. 1957;15:164–196.
8. Burke AP, Farb A, Virmani R. The pathology of primary pulmonary hypertension. *Modern Pathol*. 1991;4:269–282.
9. Pump KK. Distribution of bronchial arteries in the human lung. *Chest*. 1972;62:447–451.
10. Wagenvoort CA. Lung biopsy specimens in the evaluation of pulmonary vascular disease. *Chest*. 1980;77:614–625.
11. Heath D. The pathology of pulmonary hypertension. *Eur Respir Rev*. 1993;16:555–558.
12. Kanjuh VI, Fellers RD, Edwards JE. Pulmonary vascular plexiform lesions. *Arch Pathol*. 1964;78:513–522.
13. Roberts WC. A simple histologic classification of pulmonary arterial hypertension. *Am J Cardiol*. 1986;58:385–386.
14. Pump KK. The bronchial arteries and their anastomoses in the human lung. *Dis Chest*. 1963;43:245–255.
15. Marchand P, Gilroy JC, Wilson VH. An anatomical study of the bronchial vascular system and its variations in disease. *Thorax*. 1950;5:207–221.
16. Hasegawa I, Kobayashi K, Kohda E, Hiramatsu K. Bronchopulmonary arterial anastomoses at the precapillary level in human lung: visualization using CT angiography compared with microangiography of autopsied lung. *Acta Radiol*. 1999;39:578–584.
17. Rabinovitch M, Herrera-DeLeon V, Castaneda AR, Reid L. Growth and development of the pulmonary vascular bed in patients with tetralogy of fallot with or without pulmonary atresia. *Circulation*. 1981;64: 1234–1249.
18. Yaginuma G-Y, Hohri H, Takahashi T. Distribution of arterial lesions and collateral pathways in the pulmonary hypertension of congenital heart disease: a computer aided reconstruction study. *Thorax*. 1990;45: 586–590.
19. Hopkins WE. Severe pulmonary hypertension in congenital heart disease: a review of Eisenmenger syndrome. *Curr Opin Cardiol*. 1995;10: 517–523.
20. Perloff JK. Ventricular septal defect. In: Perloff JK. *Clinical Recognition of Congenital Heart Disease,* 5th ed. Philadelphia: WB Saunders Co; 2003:311–347.
21. Wood P. The Eisenmenger syndrome or pulmonary hypertension with reversed central shunt. *BMJ*. 1958;2:701–709.
22. Cheah FK, Sheppard MN, Hansell DM. Computed tomography of diffuse pulmonary haemorrhage, with pathological correlation. *Clin Radiol*. 1993;48:89–93.
23. Primack SL, Miller RR, Müller NL. Diffuse pulmonary hemorrhage: clinical pathologic and imaging features. *AJR Am J Radiol*. 1995;2: 295–300.
24. Perloff JD, Rosove MH, Child JS, Wright GB. Adults with cyanotic congenital heart disease: hematologic management. *Ann Intern Med*. 1988;109:406–413.
25. Hansell DM. Small vessel diseases of the lung: CT-pathologic correlates. *Radiology*. 2002;225:639–653.